



OPEN

Biosynthesis and characterization of silver nanoparticles from *Punica granatum* (pomegranate) peel waste and its application to inhibit foodborne pathogens

Salma M. Farouk¹, Samah H. Abu-Hussien^{2✉}, Basma T. Abd-Elhalim², Reham M. Mohamed¹, Naira M. Arabe¹, Ahmed A. T. Hussain¹, Mostafa E. Mostafa¹, Bahaa Hemdan³, Salwa M. El-Sayed⁴, Ashraf Bakry⁵, Naglaa M. Ebeed⁵, Mahmoud Salah^{6,7}, Hesham Elhariry⁸ & Ahmed Galal⁹

Polyphenolics have been predicted to effectively develop antimicrobial agents for the food industry as food additives and promote human health. This study aims to synthesize pomegranate peel extract (PPE) with silver nanoparticles (AgNPs) against eight foodborne pathogens. Multispectroscopic analysis of UV–vis spectroscopy, Zeta potential, Fourier transform infrared (FTIR) and scanning electron microscopy (SEM) analysis were used to characterize the interaction between PPE and AgNPs. Eight foodborne pathogenic strains (six bacterial and two fungal strains) *Bacillus subtilis* ATCC 6633, *Enterococcus faecalis* ATCC 29212, *Escherichia coli* ATCC 8379, *Klebsiella pneumoniae* ATCC 00607, *Salmonella typhi* DSM 17058, *Shigella sonnei* DSM 5570, *Aspergillus flavus* ATCC 9643, and *Rhizopus oryzae* ATCC 96382 were used to test the inhibitory potential of PPW-AgNPs. The reaction colour of PPE-AgNPs from yellow to brown indicated that the nanoparticles were successfully formed. The UV absorption of PPE-AgNPs was detected at 440 nm of 0.9 SPR. SEM image of PPE-AgNPs exhibited spherical shapes with a zeta potential of – 20.1 mV. PPE-AgNPs showed high antimicrobial activity against all tested strains. The highest inhibition activity of PPE-AgNPs was recorded for the *B. subtilis* strain followed by *K. pneumoniae*, while the highest resistance was noticed for *R. oryzae*. The components of pomegranate peel were analyzed using gas chromatography–mass spectrometry (GC–MS). The major constituents of pomegranate peel is phenol (51.1%), followed by Isocitronellol (19.41%) and 1-Propanol, 2-(2-hydroxypropyl)- (16.05%). PPE is key in the simple, eco-friendly green synthesis of extracellular stable AgNPs as an alternative source for harmful chemical disinfectants.

Food pathogenic bacteria or fungi are considered a common international health problem that causes many severe diseases and deaths worldwide. Polyphenolics have been predicted to be effective in developing antibacterial agents for the food industry as food additives and for human use. Polyphenolics inhibit the spore germination of pathogens (bacteria and fungi) in food and plants. The pomegranate (*Punica granatum* L.) is an edible

¹Undergraduate student, Biotechnology Program, Faculty of Agriculture, Ain Shams University, Hadayek Shoubra, PO Box 68, Cairo 11241, Egypt. ²Department of Agricultural Microbiology, Faculty of Agriculture, Ain Shams University, Hadayek Shoubra, PO Box 68, Cairo 11241, Egypt. ³Environmental and Climate Change Research Institute, National Research Center, Giza 1266, Egypt. ⁴Department of Biochemistry, Faculty of Agriculture, Ain Shams University, Hadayek Shoubra, PO Box 68, Cairo 11241, Egypt. ⁵Department of Genetics, Faculty of Agriculture, Ain Shams University, Hadayek Shoubra, PO Box 68, Cairo 11241, Egypt. ⁶Department of Environmental Agricultural Science, Faculty of Graduate Studies and Environmental Research, Ain Shams University, Cairo 11566, Egypt. ⁷Prevention and Detection of Microbial and Chemicals Contamination in Food Lab, School of Food and Biological Engineering, Jiangsu University, Zhenjiang 212013, Jiangsu, China. ⁸Department of Food Science, Faculty of Agriculture, Ain Shams University, Hadayek Shoubra, PO Box 68, Cairo 11241, Egypt. ⁹Department of Poultry Production, Faculty of Agriculture, Ain Shams University, Hadayek Shoubra, PO Box 68, Cairo 11241, Egypt. ✉email: samah_hashem1@agr.asu.edu.eg

fruit cultivated extensively in many tropical and subtropical nations¹. This fruit is considered beneficial to the human diet. In the pomegranate juice industry, about 50% of the weight of a pomegranate is made up of its peel, a significant source of polyphenolic compounds². Pomegranate peels were used to treat many human diseases, such as diarrhoea, vomiting, headaches, and other disorders, such as colitis, dysentery, and ulcers³. Pomegranate peel extract (PPE) has many biological activities, such as antioxidant, anti-inflammatory, and anti-carcinogenic properties, used to treat cancer, dental infections, bacterial wounds, etc. The bioactive chemicals found in pomegranate peel extract (PPE) are credited with having both antioxidant and antibacterial properties⁴. PPE is reported to contain numerous phenolic compounds, such as ellagic acid and its compounds, ellagitannins like punicalin and punicalagin, flavonoids, alkaloids, and phenolic acid, which possess antimicrobial properties^{5,6}. A study also showed that PPE provided significant amounts of bioactive chemicals, thus considered a superior antibacterial agent⁷. Developing PPE based on nanocomposites with antibacterial materials such as nanoparticles, natural polymers, and biomolecules is an important research area.

In this context, nanoparticles (NPs) have exclusive physical and chemical characteristics superior to their inhibitory potential against pathogens. AgNPs can inhibit microbial growth and foodborne pathogens such as *Staphylococcus aureus*, *Escherichia coli*, *Aspergillus niger* and *Rhizobium nigricans*⁸. AgNPs have a high surface area/volume ratio, which increases as the particle size decreases⁹. It is well known that AgNPs have the smallest size and the highest inhibitory activity against tested pathogens, but it is still unclear¹⁰. A previous study reported that triangular particles of AgNPs have higher inhibitory activity than elongated and spherical particles¹¹. The antimicrobial ability of AgNP is affected by several factors such as oxygen existence, pH and temperature¹². For instance, the acidity could enhance AgNP activity by binding to sulfur or phosphorus groups (-P, -S or -SH)¹³. In this context, the AgNP mode of action is attributed to binding with phosphorus and sulfur in the DNA structure inside the cells. Upon interaction with DNA, AgNP caused cellular leakage of metabolites, destabilization and cell death^{13,14}. Moreover, binding silver particles to the enzymes inside the cells increases reactive oxygen that denatures the cells' protein and uncontrols the transportation of ions, leading to cell death¹⁵. The biosynthesis method of AgNPs is considered an easy, quick, safe, predictable, and environmentally friendly way to fabricate well-defined sizes and morphology under optimal conditions for research¹⁵. The antimicrobial resistance (AMR) crisis has been attributed to the misuse of these drugs and the shortage of discovering new efficient and safe bio alternatives¹⁶. Therefore, the researchers resorted to producing highly efficient and environmentally friendly bio-active materials based on their antioxidant and antimicrobial properties instead of synthetic chemicals¹⁷. This study aims to evaluate pomegranate peel extract (PPE) loaded on silver nanoparticles (AgNPs) against eight foodborne pathogens. Multi-spectroscopic analysis of PPE-AgNPs driven via uv-spectroscopy, Fourier transform infrared (FTIR), particle size (nm), zeta potential (mv), poly-diversity index (Pdl), and scanning electron microscope (SEM). The Inhibition activity of PPE-AgNPs was evaluated using minimum inhibitory concentration (MIC) and minimum lethal concentration (MLC) of food pathogenic strains (six bacteria and two fungal strains) including *Bacillus subtilis* ATCC 6633, *Enterococcus faecalis* ATCC 29212, *Escherichia coli* ATCC 8379, *Klebsiella pneumoniae* ATCC 00607, *Salmonella typhi* DSM 17058, *Shigella sonnei* DSM 5570, *Aspergillus flavus* ATCC 9643, and *Rhizopus oryzae* ATCC 96382.

Materials and methods

Materials

Silver nitrate (AgNO₃) was purchased from Sigma Aldrich. Standard antibiotics (gentamicin 10.0 µg and cefuroxime 30.0 µg) were purchased from Novartis company in Egypt. Mueller–Hinton agar (MHA) media were obtained from an Elgomhoria supplier in Cairo, Egypt. Fresh pomegranate fruits were collected from local markets in Cairo, Egypt, according to the IUCN policy statement for collecting plant materials (<https://portals.iucn.org/library/efiles/documents/PP-003-En.pdf>). All chemicals were analytical grade. For used microorganisms, the antimicrobial activity of nanoparticles were tested against eight pathogenic microorganism strains including *Bacillus subtilis* ATCC 6633, *Enterococcus faecalis* ATCC 29212, *Escherichia coli* ATCC 8379, *Klebsiella pneumoniae* ATCC 00607, *Salmonella typhi* DSM 17058, *Shigella sonnei* DSM 5570, *Aspergillus flavus* ATCC 9643, and *Rhizopus oryzae* ATCC 96382. These strains were obtained from the Microbiology Department, Faculty of Agriculture, Ain Shams University. All obtained strains were maintained on glucose agar (Difco Manual, 1984) and kept in the refrigerator at 4 °C.

Standard inoculum

Standard inoculum for all tested pathogenic bacterial and fungal strains was prepared according to a previous method¹⁸. A loop of freshly prepared culture of bacterial inoculum was inoculated with 50 mL glucose broth and incubated at 37 °C for 24 h using the shake flask method at 150 rpm. The spore suspension was inoculated with a broth of malt media and incubated at 28 °C for 72 h at 150 rpm.

Preparation of pomegranate peel extract (PPE)

The pericarp was manually separated from pomegranate peels and used for extraction. According to a previous study¹⁹, the pomegranate peel aqueous extract was obtained. Twenty grams of fresh pericarp was soaked in 60.0 mL of distilled water and placed in the shaker at 150 rpm for 4 h. Samples were left in the dark at room temperature for 12 h and centrifuged at 10,000 rpm for 15 min. Supernatants were collected and used for subsequent studies.

Biosynthesis of pomegranate peel extract (PPE) loaded on silver nanoparticles (AgNps)

Fifty millilitres of AgNO₃ (1 mM) were dropwised into a glass beaker containing 2 mL of the previously prepared PPE solution (33.3% w/v in distilled water). Then, the reaction mixture was incubated overnight in the dark

using a rotary shaker incubator at 200 rpm, and the temperature was set at 30 °C (Shin Saeng, South Korea). A negative control of pomegranate extract without a silver nitrate solution was prepared. The change in colour from pale yellow to dark orange indicated the formation of the PPE-AgNPs²⁰.

Characterization of PPE-AgNPs

Appropriate characterisation techniques analysed the functional properties of the fabricated nanoparticles. The functional groups binding between AgNPs with PPE were analysed by UV–vis spectrophotometer (UV Analyst-CT 8200) in the wavelength range from 200 to 800 nm, Fourier transform infrared spectroscopy (FTIR, Shimadzu, Tracer-100) in the range of 500–4000/cm, scanning electron microscopy (FE-SEM; JOEL JSM-7800F) operated at 15 kV. The prepared PPE-AgNPs were measured using a Zeta Analyzer (NICOMPTM 380 ZLS)²¹. All characterization investigations were performed using standard methods by Creative Egyptian Biotechnologists (CEB) company, <https://www.ceb-eg.com/>, Dokki, Giza, Egypt. UV–VIS and FTIR absorption spectra of PPE and PPE-AgNPs samples were plotted using OriginPro 2022 (64-bit) SR1 v9.9.0.2 software <https://www.originlab.com/index.aspx?go=Support&pid=4440>.

Inhibitory activity of PPE-AgNPs

The antimicrobial activity of the biosynthesized PPE-AgNPs was tested against eight pathogenic microbial strains (6 bacteria and 2 fungi). *B. subtilis* ATCC 6633, *E. faecalis* ATCC 29212, *E. coli* ATCC 8379, *K. pneumoniae* ATCC 00607, *S. typhi* DSM 17058, *S. sonnei* DSM 5570, *A. flavus* ATCC 9643, and *R. oryzae* ATCC 96382 were grown on MHA and malt agar media, respectively. Well diffusion method was used to test the inhibitory effect²² of eight different concentrations of PPE-AgNPs against the eight microbial strains. Briefly, 50.0 µL of each microbial inoculum (10⁶ CFU/mL) was spread separately onto the surface of MHA agar plates. Wells were made using a sterilized cork porer 6 mm in diameter then filled with 0.1 mL of PPE-AgNPs in different concentrations (1000, 500, and 250, 125, 75, and 25 µg/mL) using ampicillin and streptomycin 1000 µg/mL as a positive control. All plates were incubated at 37 °C and 28 °C for 24 h and 72 h for bacteria and fungi, respectively. The zone of inhibition around each well was measured using a ruler and expressed by centimetre as IZD (cm)²³.

Activity index was calculated according to²⁴ which was obtained by comparing the diameter of the inhibition zone of PPE-AgNPs with the standard reference antibiotic according to the following equation:

$$\text{Activity index (AI)} = \text{IZD of AgNPs} / \text{IZD of reference antibiotic}$$

Minimum inhibitory concentration (MIC) of PPE-AgNPs

This technique was performed according to the Clinical and Laboratory Standard Institute 17 guidelines. Shortly, Two-fold serial dilutions of 1/2, 1/4, 1/8, 1/16, 1/32, and 1/64, for the PPE-AgNPs with final concentrations of {1000 (control), 500, 250, 125, 75, 50, and 25} µg/mL were prepared and inoculated into MHA agar well plates then incubated at 37 °C and 28 °C for 24 h and 72 h for bacteria and fungi, respectively. The minimum inhibitory concentration (MIC) was defined as the lowest concentration of PPE-AgNPs that inhibits bacterial growth²¹.

Minimum lethal concentration (MLC) of PPE-AgNPs

Based on the results of MIC, Minimum lethal concentration (MLC) is expressed as the values of minimum bactericidal concentration (MBC), and minimum fungicidal concentration (MFC) is presented as the lowest AgNP concentrations inhibiting the growth of pathogenic bacterial and fungal strains. MBC value was performed by sub-culturing all negative MIC wells, then incubating at 37 °C and 28 °C for 24 h and 72 h, respectively. The least concentration that showed no growth on the growth medium was indicated as the MBC value²⁵.

PPE-AgNPs mode of action

Based on MIC, MBC and MFC results. MBC/MIC and MFC /MIC ratios were calculated. PPE-AgNPs had a bactericidal and fungicidal effect when the ratio's value is greater than or equal to 4. On the other hand, it is considered a bacteriostatic or fungistatic agent when the value equals 2 or less²⁶.

SEM preparation for the antimicrobial effect detection of PPE-AgNPs

Sterile distilled water (as control) was prepared in 50 mM PBS (pH 7.0). Subsequently, 100 µL of bacteria or fungi growth preparation (1 × 10⁶ spores or bacteria/mL) were added to each tube and incubated at 150 rpm at 30 and 28 °C for 12 and 24 h for bacteria and fungi, respectively. Then, fungi spores and bacteria were collected thrice after centrifugation (10,000 rpm, 5 min), 4 °C, and washed with 50 mM PBS (pH 7.0). Then, samples were fixed with 3% glutaraldehyde 50 mM PBS (pH 7.0) at room temperature for 4 h without agitation and rinsed with PBS four times for 20 min each. After post-fixing in 1% osmic acid at room temperature for 2 h, the samples were washed with double distilled water for 15 min. Samples were dehydrated through a graded alcohol series of 30%, 50%, 70%, 80%, 90%, and 95%, then thrice at 100% for 15 min in each series. Following this, samples were incubated in isoamyl acetate overnight. Samples were then subjected to a critical point of dry carbon dioxide and coated with gold. Observation using a scanning electron microscope (S-3400N, SEM system, Hitachi, Tokyo, Japan)²⁷.

Gas Chromatography (GC–MS) analysis for PPE

The pomegranate peel (PPE) powder was analyzed using Gas-Chromatography–Mass spectrometry (GC–MS, QQQ 7890B). 10 µL of PPE ethanolic extract were diluted with hexane (≥ 99%, Sigma–Aldrich, Darmstadt, Germany) and injection volume at 2 µL was subjected to column chromatography (Agilent 19091S-433: 1 HP-5MS,

30 m × 250 μm × 0.25 μm). The separative chromatography included QQQ Collision Cell EPC (He Quench Gas with a flow rate of 2.25 mL/min, N₂ Collision Gas with a flow rate of 1.5 mL/min) was applied. After the sample was subjected, the oven temperature was set at 40–280 °C with a flow rate of 4 °C/min and a post-run of 2 min. Qualitative volatile PPE compounds were compared with their mass involved in library data²⁸.

Statistical analysis

All samples and collected data were statistically analyzed and expressed as means using IBM® SPSS® Statistics software (2017). Tukey's test at a *P*-value of 0.05 was applied²⁹. Each experiment was performed in triplicate, and the results are expressed as mean ± SD.

Results and discussion

Biosynthesis and characterization of PPE-AgNPs

PPE-AgNP biosynthesis was detected immediately when the color changed from pale yellow to dark orange upon adding silver nitrate to the pomegranate waste extract under vigorous stirring conditions (Fig. 1). Similar color change observations have been reported in recent studies on green synthesis of silver nanoparticles using pomegranate peel extracts. In a similar study³⁰, a color change was noticed from light yellow to brown during biosynthesis of silver nanoparticles from *P. granatum* peel extract after mixing with silver nitrate solution for 20 min. A study reported a color change from pale yellow to dark brown within 1 h of mixing pomegranate peel extract and silver nitrate, indicating silver ion reduction⁵. Similarly, comparable observations were noticed of a color change from light yellow to reddish brown in 5 min after adding silver nitrate to pomegranate peel extract^{21,31}. The rapid color change from light to dark shades is attributed to the excitation of surface plasmon vibrations in the synthesized silver nanoparticles. These similar findings across recent literature validate the use of visual color change as a preliminary indicator of successful biosynthesis of silver nanoparticles using pomegranate peel extract.

UV-visible spectrophotometer

UV spectrum range were recorded for control PPE and PPE-AgNPs at 200–700 nm. Three spectrum peaks were detected for PPE control at 256.6, and 383.12 nm, while for, PPE-AgNPs, only one peak was detected with a strong surface plasmon resonance (SPR) at 440, recording a score of 0.9 (Fig. 2). Many researchers revealed the detection of AgNPs at 432–442 nm after 5 min of mixing. On the other hand, some studies reported the detection of AgNPs within 10–3 min using different peel extracts^{19,32}.

DLS and Zeta potential

PPE-AgNPs had a diameter ranging from 75.5 to 4085.6 nm with a mean size of 624.4 nm, as shown in Fig. 3 and a zeta potential of −20.1 mV, as illustrated in Fig. 4. Contrarily,³⁰ reported a much higher zeta potential of −68.93 mV and less average particle size distribution between 57.7 and 42.4 nm for the AgNPs synthesized using pomegranate peel extract. Moreover,³³ found that the average particle size of AgNPs from onion plant leaf extract was 36 nm, and the zeta potential was −24.1 mV. This wide variation in AgNP sizes is attributed to the reducing agent's structure and the chemical composition of plant leaf extract compounds³⁴. The zeta potential

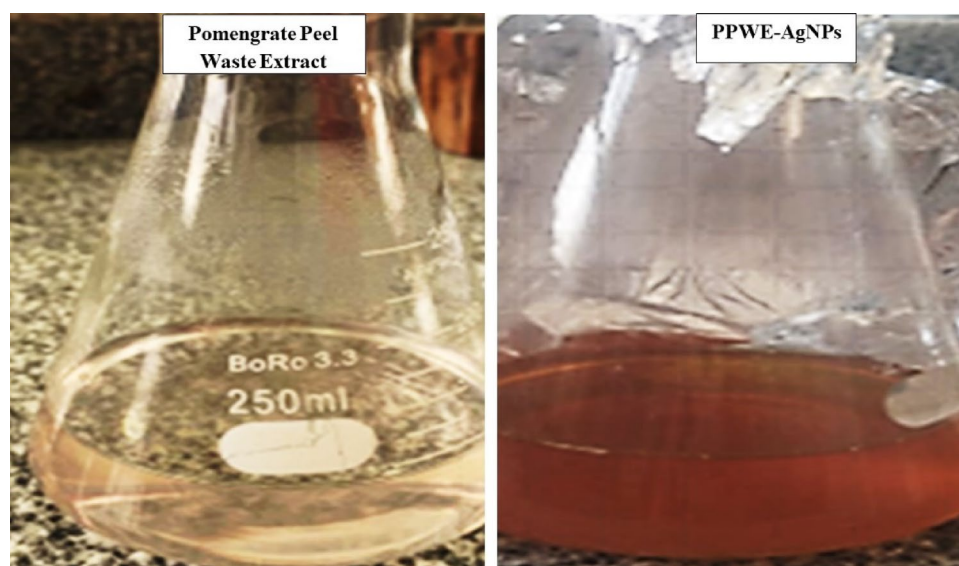


Figure 1. Colour change of PPE solution from *Punica granatum* during reduction of silver nitrate to form PPE-AgNPs. Left: pomegranate peel waste extract. Right: biosynthesis of PPE-AgNPs revealing change in colour from yellow to brown.

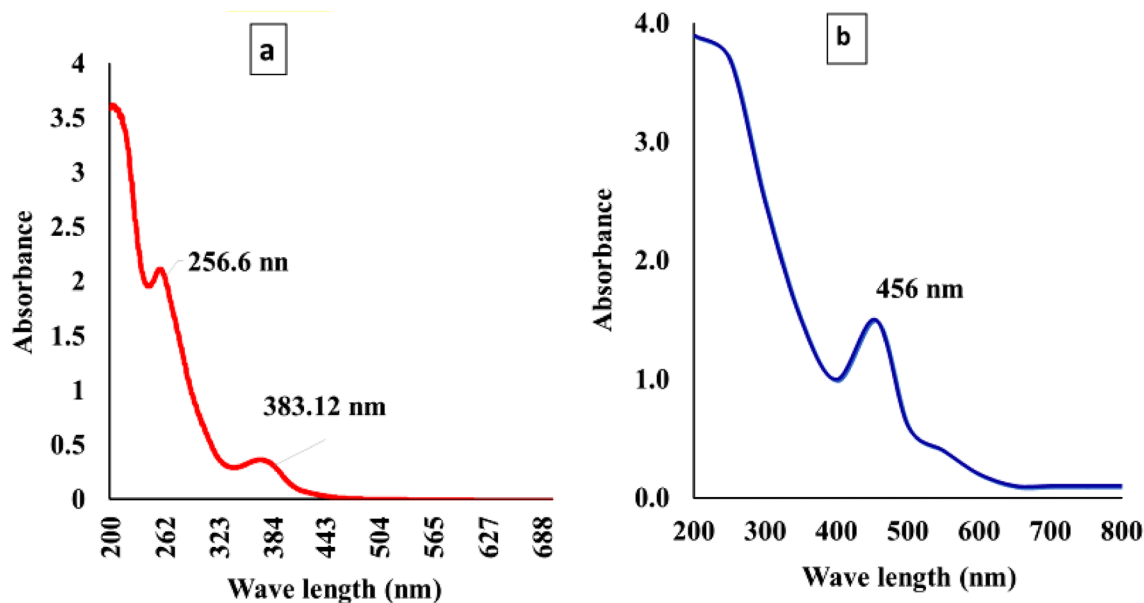


Figure 2. UV-Vis spectrum of synthesized AgNPs from *p.granatum*. (A) control treatment, (B) AgNPs from mushroom extract.

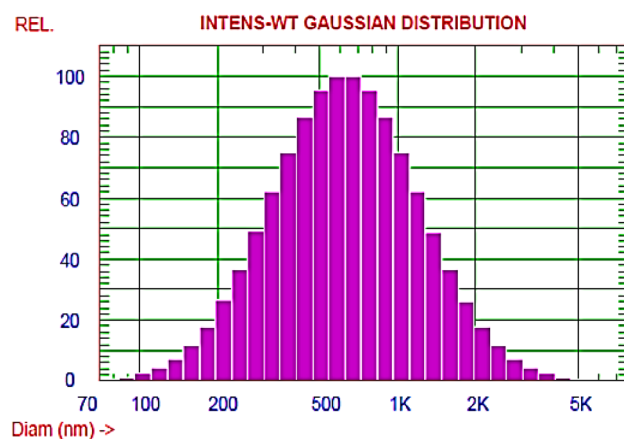


Figure 3. Dynamic light scattering (DLS) analysis for biosynthesized AgNPs from *P. granatum*.

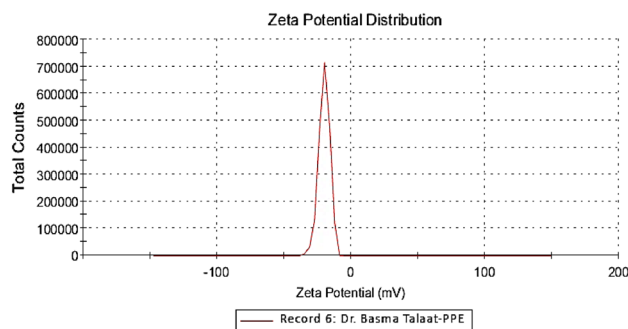


Figure 4. Zeta potential record for PPE-AgNPs from *P. granatum*.

value indicated moderate stability of biosynthesized PPE-AgNPs 0.3 mv, which could be attributed to the natural bioactive compounds responsible for capping, reduction of silver ions, and stability of nanoparticles³⁵.

Fourier transform infrared (FTIR)

FTIR was carried out to identify the main biomolecules in plant extracts that help in Ag⁺ ions reduction to AgNPs. As shown in Fig. 5 and Table 1, the main phytochemicals compounds detected in pomegranate peel waste extract were flavonoids, alkaloids, glycosides, and terpenoids. A similar study by²⁰ detected phenolic compounds in pomegranate peel waste extract using FTIR with peaks at 3371/cm, 1635/cm, 1373/cm, and 2924/cm, which were assigned to the stretching of primary and secondary amines, the C–N stretching vibrations of aromatic groups 17, respectively which play a role as capping agents.

Recent studies have comprehensively characterized the diverse phytochemicals present in pomegranate peel waste extracts that contribute to the green synthesis of metallic nanoparticles. A study³⁶ detected flavonoids, alkaloids, terpenoids and polyphenols using phytochemical tests and proposed these biomolecules reduce silver ions and stabilize nanoparticles. Specific phenolic acids like gallic acid and ellagic acid using HPLC and hypothesized these phytochemicals provide dual functions of reduction and capping in biosynthesis of gold nanoparticles³⁶.

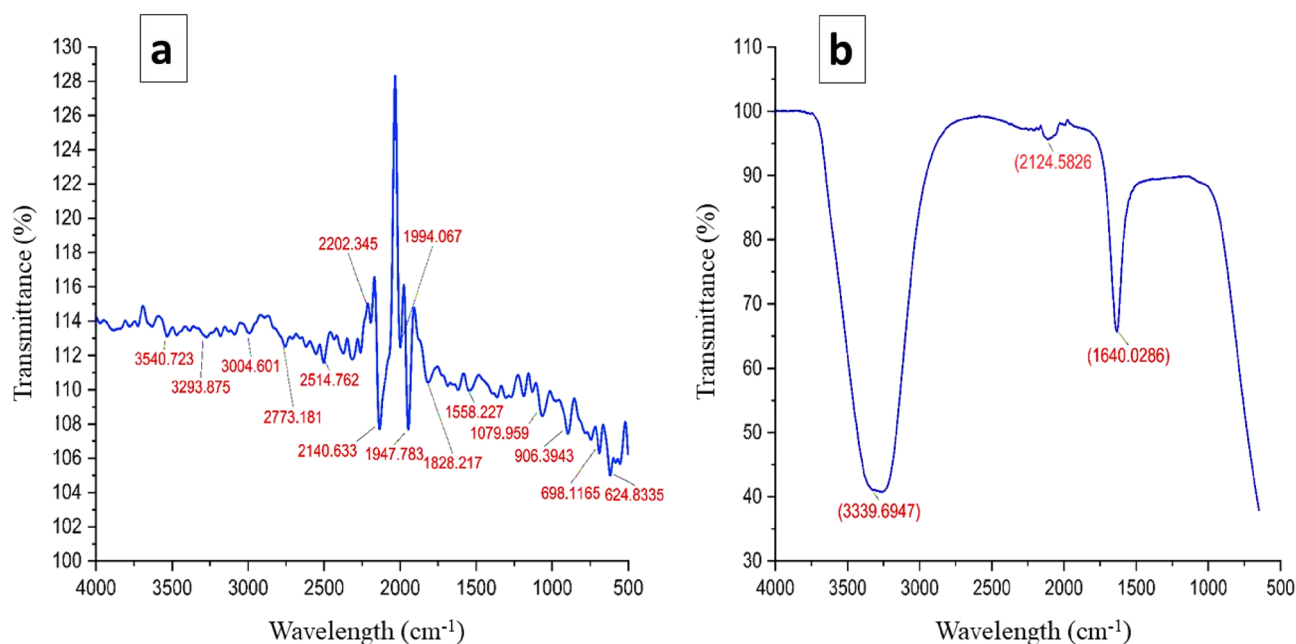


Figure 5. FTIR spectrum of biosynthesized PPE-AgNPs from *P. granatum* by reduction of Ag⁺ ions. (A) Before AgNPs biosynthesis, (B) after the AgNPs biosynthesis.

No.	Intensity	Peak position	Functional group	Compound
1	3272.25	3333–3267	C–H stretch	Alkyne
2	2502.81	3300–2500	O–H stretch	Carboxylic acid
3	2192.50	2260–2190	C≡C stretch	Alkyne
4	2135.48	2145–2120	N=C=N stretch	Carbodiimide
5	1999.17	2140–1990	N=C=S stretch	Isothiocyanate
6	1946.18	2000–1900	C=C=C stretch	Alkene
7	1816.53	1815–1770	C=O stretch	Acid chlorides
8	1618.32	1620–1610	C=C stretch	α, β-unsaturated ketone
9	1545.90	1570–1490	NO ₂ Stretch	Nitro compounds
10	1303.72	1400–1000	C–F Stretch	Alkyl & Aryl halides
11	1186.92	1400–1000	C–F stretch	Alkyl & Aryl halides
12	1065.15	1400–1000	C–F stretch	Alkyl & Aryl halides
13	895.63	900–680	C–H bend	Aromatic compounds
14	689.20	900–680	C–H bend	Aromatic compounds
15	619.20	840–600	C–Cl bend	Alkyl & Aryl halides
16	500.14	600–500	C–I stretch	Aryl halides

Table 1. FTIR analysis of biosynthesized PPE-AgNPs from *P. granatum*.

Detected peaks at 3396, 3278, and 3169/cm that were attributed to various (OH) and (NH) groups as well as H-bonding water–OH, alcohols, and amides that possibly are a part of NPs-stabilizing compounds, and the capping agents. Hence, it is reported that the amide group, amino, carbonyl group, and polyphenolic compounds in the PPE are a part of the redox reaction, dispersion, capping, and stabilizers involved in the production of nanoparticles during the process of synthesis³⁷. In summary, these recent studies strongly indicate the diverse phytochemical composition of pomegranate peel that provides reducing, capping and stabilizing agents for green sustainable of nanoparticle synthesis.

Scanning electron microscope (SEM)

Scanning Electron Microscopy (SEM) determined the PPE-AgNP's shape and size from *Punica granatum*. SEM analysis showed semi-spherical coated AgNPs, as shown in Fig. 6.

Inhibitory activity of PPE-AgNPs from *Punica granatum*

Antibiotic susceptibility test of the biosynthesized PPE-AgNPs was performed using eight foodborne pathogens, including six bacterial and two fungal strains. Data in Table 2 showed that all tested pathogenic bacteria were highly sensitive to AgNPs with IZD ranging from 4.5 to 0.96 cm, while fungi were resistant with the lowest IZD of 0.96 cm when compared to the control antibiotic drug with IZD scored 4.1–0.96 cm. The most sensitive bacterial strain was recorded for *B. subtilis* with an IZD of 4.5 cm and activity index (AI) of 1.10. However, the lowest IZD and activity index (AI) was observed for the fungal strains of *A. flavus* and *R. oryzae* ATCC 96382, reaching 1.30 and 0.96 with AI of 0.48 and 0.51, respectively. This inhibitory activity is attributed to the binding of silver to the phospholipid layer of the bacterial cell membrane, where the formation of pores occurs. This,

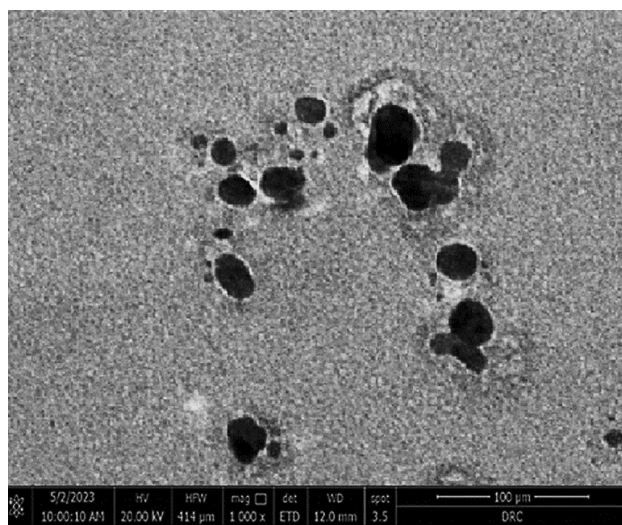


Figure 6. Scanning Electron Microscope (SEM) indicating the biosynthesized PPE-AgNPs from *P. granatum*.

Pathogen strains	Inhibition zone diameter (cm)		AI
	Antibiotic (1000 μg/mL)	PPE-AgNPs (1000 μg/mL)	
G⁺ve Bacteria			
<i>B. subtilis</i> ATCC 6633	4.10 ^b ± 0.41	4.5 ^a ± 0.41	1.10
<i>E. faecalis</i> ATCC 29212	0.96 ^g ± 0.22	2.5 ^d ± 0.55	2.60
G⁻ve Bacteria			
<i>E. coli</i> ATCC 8379	0.98 ^g ± 0.16	2.0 ^e ± 0.14	2.05
<i>K. pneumoniae</i> ATCC 00607	1.30 ^g ± 0.65	2.5 ^d ± 0.77	1.92
<i>S. typhi</i> DSM 17058	0.96 ^h ± 0.02	2.6 ^d ± 0.11	2.70
<i>S. sonnei</i> DSM 5570	0.98 ^h ± 0.04	2.5 ^d ± 0.30	2.55
Fungi			
<i>A. flavus</i> ATCC 9643	2.77 ^c ± 0.02	1.30 ^g ± 0.84	0.48
<i>R. oryzae</i> ATCC 96382	1.88 ^{cd} ± 0.50	0.96 ^h ± 0.45	0.51

Table 2. Inhibitory activity PPE-AgNPs expressed as zone diameter (IZD) and activity index (AI). Standard antibiotics were streptomycin, ampicillin, and fluconazole against G⁺ve bacteria, G⁻ve bacteria and fungi, respectively.*mm, milli meter; AI, activity index; and SE (±), standard error. Values in the same column followed by the same letter are not significantly different, according to²⁹ at a 5% level.

in turn, results in their destabilization and an increase in membrane permeability, causing leakage of cellular metabolites and cell death^{30,38}. Also,³⁴ found that the AgNPs synthesized using pomegranate fruit peel extract as a reducing agent exhibited a fairly significant inhibition with 2.6 cm against *S. aureus*. The major mechanism of silver nanoparticles manifesting antibacterial properties was anchoring or penetrating the bacterial cell wall and modulating cellular signalling by dephosphorylating peptide substrate on tyrosine residues.

Minimum inhibition concentration (MIC) of PPE-AgNPs

MIC values of PPE-AgNPs against the tested pathogenic bacterial and fungal strains ranged from 1000 to 12.5 µg/mL, as illustrated in Table 3. The MIC value was exhibited at 250 µg/mL for *E. coli* ATCC 8379 and *E. faecalis* ATCC 29212, while it was 125 µg/mL *K. pneumoniae*. On the other hand, it was 50 µg/mL against *S. typhi* and 25 µg/mL against *B. subtilis*. The results showed 100% of the antibacterial spectrum activity of PPE-AgNPs at concentrations ranging from 1000 to 250 µg/mL, whereas at concentrations of 125, and 75 µg/mL the activity was 66.7% and 50%, respectively. Whereas at a concentration of 50 µg/mL, the antibacterial spectrum showed 33.3%; at a 25 µg/mL concentration, it exhibited 16.6% activity. There was no antibacterial spectrum at 12.5 µg/mL. The PPE-AgNPs MIC antifungal activity investigation was at concentrations of 1000–12.5 µg/mL, both *A. flavus* and *R. oryzae*. The MIC was 250 µg/mL for *R. oryzae* and 75 µg/mL for *A. flavus*. At 1000–250 µg/mL concentrations, 50% of the spectrum of activity was attained for all fungi at 125–75 µg/mL. In addition, concentrations ranging from 25 to 12.5 µg/mL did not display any activity against the tested fungal strains.

Minimum lethal concentration (MLC) of PPE-AgNPs

The minimum lethal concentration MLC (MBC and MFC) for pomegranate peel silver nanoparticles (PPE-AgNPs) are presented in Table 4. The MBC value was 500 µg/mL for *E. coli*, *E. faecalis* and *K. pneumoniae*. On the other hand, it was 250 µg/mL for *S. sonnei* and 125 µg/mL for *S. typhi* and *B. subtilis*. The results showed 100% of the antibacterial spectrum activity of PPE-AgNPs at concentrations ranging from 1000 to 250 µg/mL, whereas at concentrations of 250–125 µg/mL, the activity was 33.3%. There was no antibacterial spectrum at a 75–12.5 µg/mL concentration. The MFC was 1000 µg/mL for *R. oryzae* ATCC 96382, while it was 500 µg/mL for *A. flavus*, as shown in Table 4. At the concentration 1000, the spectrum activity was 100%, while at 500 µg/mL, only 50% of the activity was attained for all fungi at 250–12.5 µg/mL did not display any activity against the tested fungal strains.

Pomegranate peels silver nanoparticles (PPE-AgNPs) action mode

Finally, it could be observed that the mode of action of PPE-silver nanoparticles against pathogenic bacterial and fungal strains is shown in Table 5. Results indicated that the PPE-AgNPs have a bactericidal against *E. coli* and *E. faecalis*, while it was bacteriostatic with *B. subtilis*, *K. pneumoniae*, *S. typhi*, *S. sonnei*, and *S. sonnei*. Also, it revealed a fungistatic effect for both fungal strains. In Brief, PPE-AgNPs showed high antimicrobial activity against all tested strains. The highest inhibition activity of PPE-AgNPs was recorded for the *B. subtilis* strain followed by *K. pneumoniae*, while the highest resistance was noticed for *R. oryzae*, Fig. 7. Previous research has elucidated the complex interactions between nanoparticles (NPs) and microorganisms including bacteria, fungi and viruses along with the resultant antimicrobial effects. Metal NPs like silver, gold, zinc oxide and copper have shown pronounced antibacterial activity against both Gram positive and Gram negative bacteria due to their positively charged surfaces interacting and damaging the negatively charged bacterial cell membrane leading to cell death^{39,40}. The antimicrobial mechanisms involve generation of reactive oxygen species, inhibition of vital

Pathogenic bacteria	MIC (µg/mL) of PPE-AgNPs							
	1000 (control)	500	250	125	75	50	25	12.5
<i>B. subtilis</i> ATCC 6633	–	–	–	–	–	–	–	+
<i>E. faecalis</i> ATCC 29212	–	–	–	+	+	+	+	+
<i>E. coli</i> ATCC 8379	–	–	–	+	+	+	+	+
<i>K. pneumoniae</i> ATCC 00607	–	–	–	–	+	+	+	+
<i>S. typhi</i> DSM 17058	–	–	–	–	–	–	+	+
<i>S. sonnei</i> DSM 5570	–	–	–	–	–	+	+	+
Spectrum of activity (%)	6/6	6/6	6/6	4/6	3/6	2/6	1/6	0/6
	100	100	100	66.7	50.0	33.3	16.6	0
Pathogenic fungi	MIC (µg/mL) of PPE-AgNPs							
	1000 (control)	500	250	125	75	50	25	12.5
<i>A. flavus</i> ATCC 9643	–	–	–	–	–	+	+	+
<i>R. oryzae</i> ATCC 96,382	–	–	–	+	+	+	+	+
Spectrum of activity (%)	2/2	2/2	2/2	1/2	1/2	0/2	0/2	0/2
	100	100	100	50	50	0.00	0.00	0.00

Table 3. Minimum inhibitory concentration (MIC) of PPE-AgNPs against foodborne pathogens. –, no growth; +, growth.

Pathogenic bacteria	MBC ($\mu\text{g/mL}$) of PPE-AgNPs							
	1000 (control)	500	250	125	75	50	25	12.5
<i>B. subtilis</i> ATCC 6633	–	–	–	–	+	+	+	+
<i>E. faecalis</i> ATCC 29212	–	–	+	+	+	+	+	+
<i>E. coli</i> ATCC 8379	–	–	+	+	+	+	+	+
<i>K. pneumoniae</i> ATCC 00607	–	–	+	+	+	+	+	+
<i>S. typhi</i> DSM 17058	–	–	–	–	+	+	+	+
<i>S. sonnei</i> DSM 5570	–	–	–	+	+	+	+	+
Spectrum of activity (%)	6/6	6/6	2/6	2/6	0/6	0/6	0/6	0/6
	100	100	33.3	33.3	0	0	0	0
Pathogenic fungi	MFC ($\mu\text{g/mL}$) of PPE-AgNPs							
	1000 (control)	500	250	125	75	50	25	12.5
<i>A. flavus</i> ATCC 9643	–	–	+	+	+	+	+	+
<i>R. oryzae</i> ATCC 96382	–	+	+	+	+	+	+	+
Spectrum activity (%)	2/2	1/2	0/2	0/2	0/2	0/2	0/2	0/2
	100	50	0.00	0.00	0.00	0.00	0.00	0.00

Table 4. Minimum lethal concentration (MLC) of PPE-AgNPs against foodborne pathogens. –, no growth, +, growth.

Pathogenic bacteria	MIC (PPE-AgNPs $\mu\text{g/mL}$)	MLC (PPE-AgNPs $\mu\text{g/mL}$)	MLC/MIC ratio	Mode of action
Bacteria				
<i>E. faecalis</i> ATCC 29212	250	500	2.0	+
<i>E. coli</i> ATCC 8379	250	500	2.0	+
<i>B. subtilis</i> ATCC 6633	25	125	5.0	–
<i>K. pneumoniae</i> ATCC 00607	125	500	4.0	–
<i>S. typhi</i> DSM 17058	50	125	2.5	–
<i>S. sonnei</i> DSM 5570	75	250	3.3	–
Fungi				
<i>A. flavus</i> ATCC 9643	75	500	6.6	–
<i>R. oryzae</i> ATCC 96382	250	1000	4.0	–
Bactericidal/Fungicidal (+) = ≤ 2 and Bacteriostatic/fungistatic (–) effect = ≥ 4				

Table 5. Minimum inhibitory concentration (MIC) and minimum lethal concentration (MLC) of PPE-AgNPs against foodborne pathogens.

microbial enzymatic and protein functions, and disruption of DNA replication and protein synthesis causing growth inhibition. Factors like NP size, shape, surface properties and concentration influence the antibacterial effects, with smaller NPs having greater impacts due to higher surface area to volume ratios⁴¹. However, some studies have reported microbial resistance development against NPs indicating dynamic interactions and adaptation. Overall, previous research has clearly demonstrated the broad-spectrum antimicrobial properties of diverse NPs and elucidated their complex interactions with microbial cells that induce cell damage and growth inhibition. But microbial adaptation mechanisms point to the need for further studies on these evolving NP-microbe interactions.

SEM preparation for the antimicrobial effect detection of PPE-AgNPs

In our SEM findings, obvious signs of differences in cell morphology between control and treated cells with damage to the cell wall for the most influenced microorganisms of *Bacillus subtilis*, *Enterococcus faecalis*, and *Aspergillus niger* were found according to analysis with the aid of a scanning electron microscope (SEM). After 12

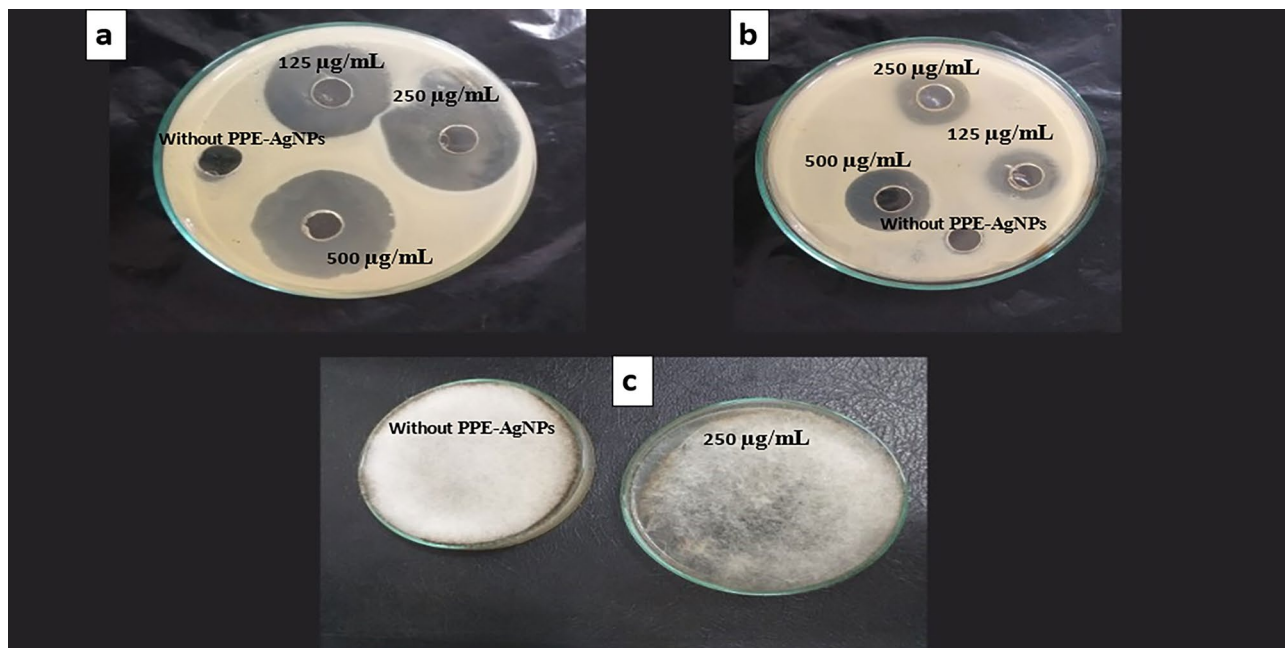


Figure 7. Antimicrobial activity of PPE-AgNPs against the most sensitive pathogenic strains, (a) *B. subtilis*, (b) *K. pneumonia*, (c) *R. oryzae*.

and 24 h of incubation at 30 and 28 °C for 12 and 24 h for bacteria and fungi, respectively. The control microbes treated with distilled water displayed a normal and compact morphology (Fig. 8a, b, e), whereas the microbial cells treated with 1000 µg/mL PPE-AgNPs showed irregular modifications. As shown in Fig. 8c, d, cell surfaces appeared to suffer from PPE-AgNPs with irregular morphological shapes, disrupted cell walls and pores or invaginations on cells, and hypha broken down for fungi, as shown in Fig. 8f, g. In the same line, it was found that AgNPs, there was accumulation on *S. aureus* and *P. aeruginosa* cell surface, which results in pores or invaginations on cells that affect bacterial viability^{27,42}. Cells treated with AgNPs showed destruction and distortion at cell poles due to an accumulation of nanoparticles that affected cell viability and caused cell death and pores or invaginations on cells. The antifungal SEM investigation⁴³ shows a great variation between a control with the normal shape of fungal mycelium, whereas the treated sample with AgNPs shows aggregations of small micro nanoparticles at an earlier stage of formation on the hyphae⁴⁴.

Gas Chromatography (GC–MS) analysis for PPE

The phytochemical composition of pomegranate peel (PPE) was analyzed using GC–MS and presented in Table 6 and Fig. 9. The major constituents of pomegranate peel were phenol (51.1%), followed by Isocitronellol (19.41%) and 1-Propanol, 2-(2-hydroxypropyl)- (16.05%). Additionally, other terpenoids such as geraniol (4.89%), styrene (4.47%), and isopolygol (4.07%) have been identified in the ethanolic extract of pomegranate peel (Fig. 9). Geraniol is a monoterpene alcohol with a pleasant rose-like aroma, is found in many essential oils and has antibacterial and antifungal potential^{45,46}. Phenolic compounds have gained attention, especially in the food research sector, as microbial growth inhibitors for foodborne pathogenic and spoilage bacteria. All phenols also have promising anti-quorum sensing potential and inhibit the biofilm formation and toxin production of food-related pathogens⁴⁷.

Conclusion

The present study demonstrates a simple, eco-friendly biosynthesis of PPE-AgNPs using pomegranate peel extract as a reducing agent. The phytochemicals detected by the FTIR, such as flavonoids, alkaloids, glycosides, and terpenoids, acted as better reducing and capping agents. Besides the physicochemical advantages of PPE-AgNPs, these have shown improved antimicrobial activity, which can contribute to solving the global problem of multi-drug resistant (MDR) microorganisms soon.

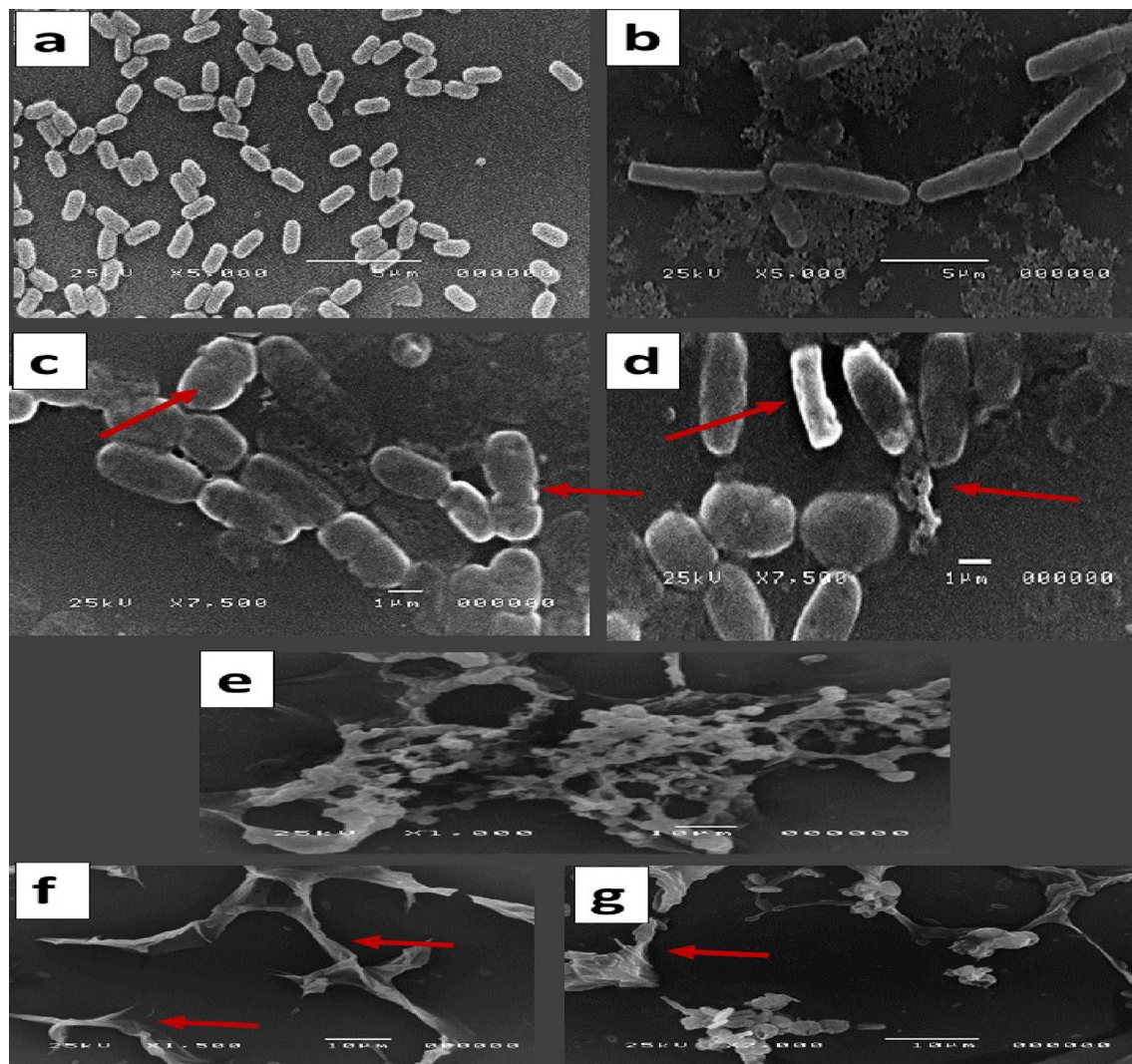


Figure 8. SEM images of (a) *Bacillus subtilis*, (b) *Enterococcus faecalis*, and (e) *Aspergillus niger* cells control treated with distilled water, while (c) *Bacillus subtilis*, (d) *Enterococcus faecalis*, and (e, f) *Aspergillus niger* cells treated with 1000 µg/mL PPE-AgNPs. Arrows refer to the morphologic alterations in cells and contact of PPE-AgNPs cell membrane and collapsed cell walls.

No. peak	Component names	RT ^a (min)	Percentage (%) ^b
1	Styrene	8.241	4.47
2	Isopolygol	21.242	4.07
3	Geraniol	22.376	4.89
4	1-Propanol, 2-(2-hydroxypropoxy)-	25.681	16.05
5	Phenol	26.312	51.1
6	Isocitronellol	35.308	19.41

Table 6. Chemical composition (%) of PPE analyzed by GC-MS. ^aRetention time. ^bCompound percentage.

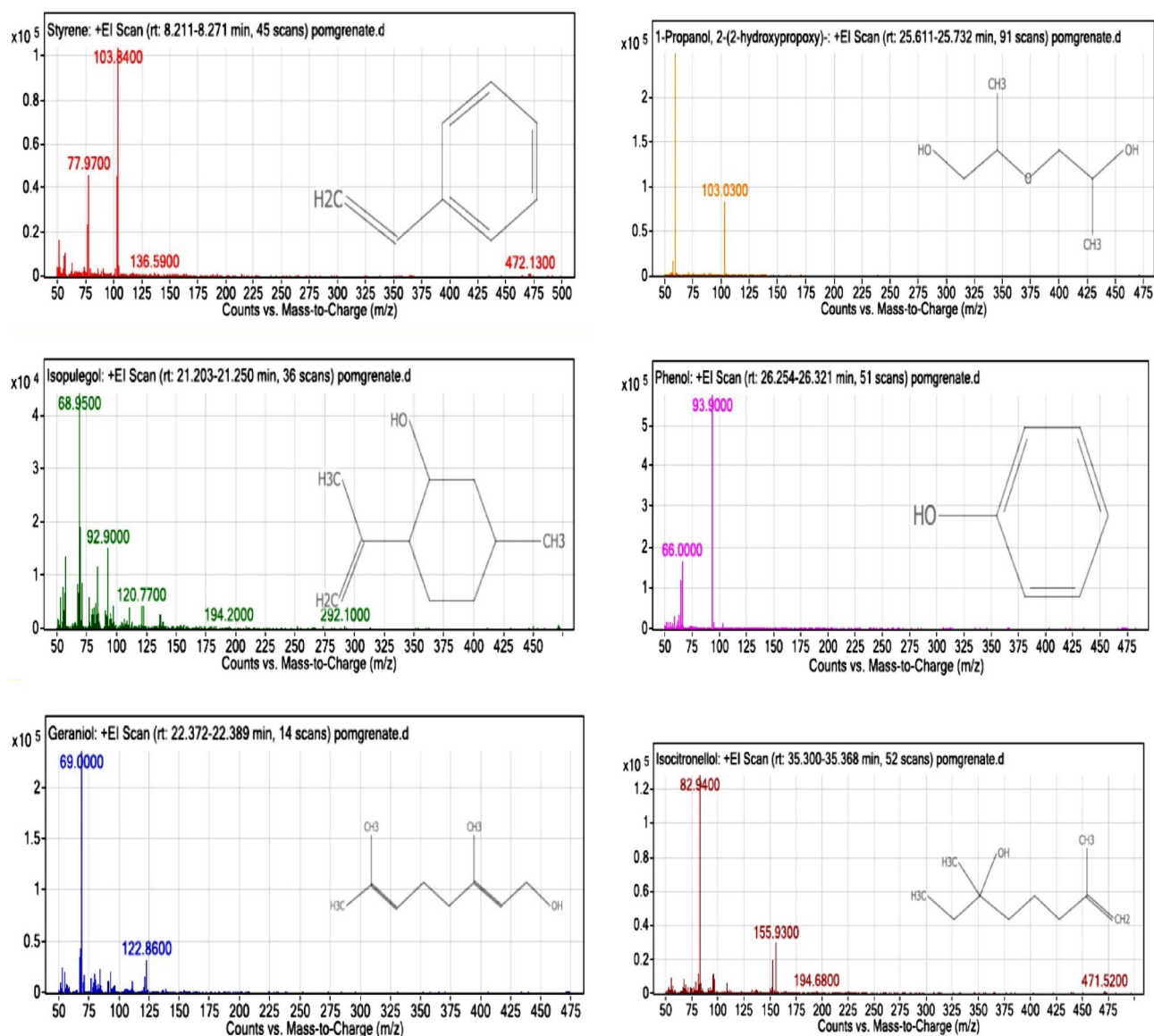


Figure 9. Chromatographic analysis of bioactive compounds in pomengrate peel (PPE).

Data availability

The raw and analyzed data used during the current study are available from the corresponding author upon reasonable request. All microbial pathogens were provided by the Agricultural Microbiology Department, Faculty of Agriculture, Ain Shams University, Cairo, Egypt and were deposited in the following strain providers (1) *B. subtilis* ATCC 6633 was from ATCC collection <https://www.atcc.org/products/6633>. (2) *E. fecalis* ATCC 29,212 was from the ATCC collection <https://www.atcc.org/products/29212>. (3) *E. coli* ATCC 8379 was from ATCC collection <https://www.atcc.org/products/8379> and was deposited in GenBank with taxonomy ID: NCBI:txid 481805 https://www.ncbi.nlm.nih.gov/Taxonomy/Browser/wwwtax.cgi?TPE-AgNPs_id=481805. (4) *K. pneumoniae* ATCC 00607 was from ATCC collection <https://www.atcc.org/products/00607>. (5) *S. typhi* DSM 17058 was from DSM collection <https://www.dsmz.de/collection/catalogue/details/culture/DSM-17058>. (6) *S. sonii* DSM 5570 was from DSM collection <https://www.dsmz.de/collection/catalogue/details/culture/DSM-5570>. (7) *A. flavus* ATCC 9643 was from ATCC collection <https://www.atcc.org/products/9643>. (8) *R. oryzae* ATCC96382 was from ATCC collection <https://www.atcc.org/products/96382>. (9) Policy of plant materials collection <https://portals.iucn.org/library/efiles/documents/PP-003-En.pdf>.

Received: 3 July 2023; Accepted: 31 October 2023

Published online: 09 November 2023

References

- Seeram, N. P. *et al.* In vitro antiproliferative, apoptotic and antioxidant activities of punicalagin, ellagic acid and a total pomegranate tannin extract are enhanced in combination with other polyphenols as found in pomegranate juice. *J. Nutr. Biochem.* **16**, 360–367 (2005).
- Bachoual, R., Talmoudi, W., Boussetta, T., Braut, F. & El-Benna, J. An aqueous pomegranate peel extract inhibits neutrophil myeloperoxidase in vitro and attenuates lung inflammation in mice. *Food Chem. Toxicol.* **49**, 1224–1228 (2011).
- Ul-Islam, M. *et al.* Development of low-cost bacterial cellulose-pomegranate peel extract-based antibacterial composite for potential biomedical applications. *Int. J. Biol. Macromol.* **231**, 1232 (2023).
- Mohanta, Y. K. *et al.* Nanotechnology in combating biofilm: A smart and promising therapeutic strategy. *Front. Microbiol.* **13**, 748. <https://doi.org/10.3389/fmicb.2022.1028086> (2022).
- Gullon, B., Pintado, M. E., Pérez-Álvarez, J. A. & Viuda-Martos, M. Assessment of polyphenolic profile and antibacterial activity of pomegranate peel (*Punica granatum*) flour obtained from co-product of juice extraction. *Food Control* **59**, 94–98 (2016).
- Sharifi-Rad, M. *et al.* Variation of phytochemical constituents, antioxidant, antibacterial, antifungal, and anti-inflammatory properties of *Grantia aucheri* (Boiss.) at different growth stages. *Microb. Pathog.* **172**, 1058 (2022).
- Mohanta, Y. K. *et al.* Anti-biofilm and antibacterial activities of silver nanoparticles synthesized by the reducing activity of phytoconstituents present in the Indian medicinal plants. *Front. Microbiol.* **11**, 330 (2020).
- Hamida, R. S., Ali, M. A., Goda, D. A., Khalil, M. I. & Al-Zaban, M. I. Novel biogenic silver nanoparticle-induced reactive oxygen species inhibit the biofilm formation and virulence activities of methicillin-resistant *Staphylococcus aureus* (MRSA) strain. *Front. Bioeng. Biotechnol.* **8**, 12 (2020).
- Mohanta, Y. K. *et al.* Silver nanoparticles synthesized using wild mushroom show potential antimicrobial activities against food borne pathogens. *Molecules* **23**, 655 (2018).
- Al-Wrafy, F. A., Al-Gheethi, A. A., Ponnusamy, S. K., Noman, E. A. & Fattah, S. A. Nanoparticles approach to eradicate bacterial biofilm-related infections: A critical review. *Chemosphere* **288**, 1326 (2022).
- Thammawithan, S. *et al.* A biological study of anisotropic silver nanoparticles and their antimicrobial application for topical use. *Vet. Sci.* **8**, 17 (2021).
- Parandhaman, T. *et al.* Antimicrobial behavior of biosynthesized silica-silver nanocomposite for water disinfection: A mechanistic perspective. *J. Hazard Mater.* **290**, 117–126 (2015).
- Khatoun, N., Sharma, Y., Sardar, M. & Manzoor, N. Mode of action and anti-Candida activity of *Artemisia annua* mediated-synthesized silver nanoparticles. *J. Mycol. Med.* **29**, 201–209 (2019).
- Majeed, S. *et al.* Bioengineering of green-synthesized TAT peptide-functionalized silver nanoparticles for apoptotic cell-death mediated therapy of breast adenocarcinoma. *Talanta* **253**, 124026 (2023).
- Saratale, R. G. *et al.* New insights on the green synthesis of metallic nanoparticles using plant and waste biomaterials: Current knowledge, their agricultural and environmental applications. *Env. Sci. Pollut. Res.* **25**, 10164–10183 (2018).
- Uddin, T. M. *et al.* Antibiotic resistance in microbes: History, mechanisms, therapeutic strategies and future prospects. *J. Infect. Public Health* **14**, 1750–1766. <https://doi.org/10.1016/j.jiph.2021.10.020> (2021).
- Tagliabue, A. & Rappuoli, R. Changing priorities in vaccinology: Antibiotic resistance moving to the top. *Front. Immunol.* **9**, 102. <https://doi.org/10.3389/fimmu.2018.01068> (2018).
- Abd-Elhalim, B. T., Gamal, R. F., Abou-Taleb, K. A. & Haroun, A. A. Biosynthesis of copper nanoparticles using bacterial supernatant optimized with certain agro-industrial byproducts. *Novel Res. Microbiol. J.* **3**, 558–578 (2019).
- Saad, P. G., Castelino, R. D., Ravi, V., Al-Amri, I. S. & Khan, S. A. Green synthesis of silver nanoparticles using Omani pomegranate peel extract and two polyphenolic natural products: Characterization and comparison of their antioxidant, antibacterial, and cytotoxic activities. *Beni Suef. Univ. J. Basic Appl. Sci.* **10**, 102 (2021).
- Abdelmigid, H. M. *et al.* Green synthesis of zinc oxide nanoparticles using pomegranate fruit peel and solid coffee grounds vs. chemical method of synthesis, with their biocompatibility and antibacterial properties investigation. *Molecules* **27**, 1236 (2022).
- Amr, M. *et al.* Utilization of biosynthesized silver nanoparticles from *Agaricus bisporus* extract for food safety application: Synthesis, characterization, antimicrobial efficacy, and toxicological assessment. *Sci. Rep.* **13**, 74 (2023).
- Murugaiyan, J. *et al.* Progress in alternative strategies to combat antimicrobial resistance: Focus on antibiotics. *Antibiotics* **11**, 200. <https://doi.org/10.3390/antibiotics11020200> (2022).
- Truong, L. B., Medina-Cruz, D., Mostafavi, E. & Rabiee, N. Selenium nanomaterials to combat antimicrobial resistance. *Molecules* **26**, 3611. <https://doi.org/10.3390/molecules26123611> (2021).
- Singariya, P., Mourya, K. K. & Kumar, P. Antimicrobial activity of the crude extracts of *Withania somnifera* and *Cenchrus setigerus* in-vitro. *Pharmacogn. J.* **4**, 60–65 (2012).
- Sales, G. *et al.* Antifungal and modulatory activity of lemon balm (*Lippia alba* (MILL.) N. E. BROWN) essential oil. *Sci. Pharm.* **90**, 31 (2022).
- Asl, A. R. *et al.* The protective effect of pomegranate peel aqueous extract on selenite-induced cataract in rats. *J. Food Biochem.* **46**, 10 (2022).
- Venkatash-Babu, G. *et al.* Enhanced method for high spatial resolution surface imaging and analysis of fungal spores using scanning electron microscopy. *Sci. Rep.* **8**, 1 (2018).
- El-Sayed, S. M. *et al.* Acaricidal and antioxidant activities of anise oil (*Pimpinella anisum*) and the oil's effect on protease and acetylcholinesterase in the two-spotted spider mite (*Tetranychus urticae* Koch). *Agric. Switzerl.* **12**, 224 (2022).
- Keselman, H. J. & Rogan, J. C. The Tukey multiple comparison test: 1953–1976. *Psychol. Bull.* **84**, 1050–1056 (1977).
- Mostafa, Y. S., Alamri, S. A., Alrumman, S. A., Hashem, M. & Baka, Z. A. Green synthesis of silver nanoparticles using pomegranate and orange peel extracts and their antifungal activity against *Alternaria solani*, the causal agent of early blight disease of tomato. *Plants* **10**, 2363 (2021).
- Saad, P. G., Castelino, R. D., Ravi, V., Al-Amri, I. S. & Khan, S. A. Green synthesis of silver nanoparticles using Omani pomegranate peel extract and two polyphenolic natural products: characterization and comparison of their antioxidant, antibacterial, and cytotoxic activities. *Beni Suef. Univ. J. Basic Appl. Sci.* **10**, 41 (2021).
- Weng, X., Yang, K., Owens, G. & Chen, Z. Biosynthesis of silver nanoparticles using three different fruit extracts: Characterization, formation mechanism and estrogen removal. *J. Environ. Manage.* **316**, 85 (2022).
- Yap, Y. H. *et al.* Green synthesis of silver nanoparticle using water extract of onion peel and application in the acetylation reaction. *Arab. J. Sci. Eng.* **45**, 4797–4807 (2020).
- Chand, K. *et al.* Green synthesis characterization and antimicrobial activity against *Staphylococcus aureus* of silver nanoparticles using extracts of neem, onion and tomato. *RSC Adv.* **9**, 17002–17015 (2019).
- Ijaz, I. *et al.* Green synthesis of silver nanoparticles using different plants parts and biological organisms, characterization and antibacterial activity. *Env. Nanotechnol. Monitor. Manag.* **18**, 1007. <https://doi.org/10.1016/j.enmm.2022.100704> (2022).
- Ritu-Verma, K. K., Das, A. & Chandra, P. Phytochemical-based synthesis of silver nanoparticle: Mechanism and potential applications. *BioNanoScience* **13**, 1359–1380. <https://doi.org/10.1007/s12668-023-01125-x> (2023).
- Zia, M. *et al.* Green synthesis of silver nanoparticles from grape and tomato juices and evaluation of biological activities. *IET Nanobiotechnol.* **11**, 193–199 (2017).

38. Mansoor, S. *et al.* Fabrication of silver nanoparticles against fungal pathogens. *Front. Nanotechnol.* **3**, 859. <https://doi.org/10.3389/fnano.2021.679358> (2021).
39. Vaid, P., Raizada, P., Saini, A. K. & Saini, R. V. Biogenic silver, gold and copper nanoparticles—a sustainable green chemistry approach for cancer therapy. *Sustain. Chem. Pharm.* **16**, 100247 (2020).
40. Gold, K., Slay, B., Knackstedt, M. & Gaharwar, A. K. Antimicrobial activity of metal and metal-oxide based nanoparticles. *Adv. Ther. (Weinh.)* **1**, 3 (2018).
41. Shaikh, S. *et al.* Mechanistic insights into the antimicrobial actions of metallic nanoparticles and their implications for multidrug resistance. *Int. J. Mol. Sci.* **20**, 2468 (2019).
42. Shaaban, M. T., Zayed, M. & Salama, H. S. Antibacterial potential of bacterial cellulose impregnated with green synthesized silver nanoparticle against *S. aureus* and *P. aeruginosa*. *Curr. Microbiol.* **80**, 2 (2023).
43. El-Wakil, D. Antifungal activity of silver nanoparticles by trichoderma species: Synthesis, characterization and biological evaluation. *Egypt J. Phytopathol.* **48**, 71–80 (2020).
44. Devi, L. S. & Joshi, S. R. Antimicrobial and synergistic effects of silver nanoparticles synthesized using: Soil fungi of high altitudes of Eastern Himalaya. *Mycobiology* **40**, 27–34 (2012).
45. de Lira, M. H. P. *et al.* Antimicrobial activity of geraniol: An integrative review. *J. Essential Oil Res.* **32**, 187–197 (2020).
46. Maczka, W., Winska, K. & Grabarczyk, M. One hundred faces of geraniol. *Molecules* **25**, 3303. <https://doi.org/10.3390/molecules25143303> (2020).
47. Takó, M. *et al.* Plant phenolics and phenolic-enriched extracts as antimicrobial agents against food-contaminating microorganisms. *Antioxidants* **9**, 165. <https://doi.org/10.3390/antiox9020165> (2020).

Acknowledgements

The authors thank the New Programs Administration, Faculty of Agriculture, Ain Shams University for providing all lab facilities.

Author contributions

B.T.A., S.M.S., B.H. and S.H.A. conceived and designed the research. S.M.F., B.T.A., S.M.S., B.H., R.M.M., N.M.A., A.A.T.H., M.E.M., S.H.A. conducted experiments and collected data. B.T.A., S.M.S., B.H., M.S. and S.H.A. analyzed and interpreted microbiological data, B.T.A., S.M.S., B.H., M.S. and S.H.A. revised manuscript. All authors wrote the draft manuscript reviewed and edited the manuscript. All authors read and approved the manuscript.

Funding

Open access funding provided by The Science, Technology & Innovation Funding Authority (STDF) in cooperation with The Egyptian Knowledge Bank (EKB).

Competing interests

The authors declare no competing interests.

Additional information

Correspondence and requests for materials should be addressed to S.H.A.-H.

Reprints and permissions information is available at www.nature.com/reprints.

Publisher's note Springer Nature remains neutral with regard to jurisdictional claims in published maps and institutional affiliations.



Open Access This article is licensed under a Creative Commons Attribution 4.0 International License, which permits use, sharing, adaptation, distribution and reproduction in any medium or format, as long as you give appropriate credit to the original author(s) and the source, provide a link to the Creative Commons licence, and indicate if changes were made. The images or other third party material in this article are included in the article's Creative Commons licence, unless indicated otherwise in a credit line to the material. If material is not included in the article's Creative Commons licence and your intended use is not permitted by statutory regulation or exceeds the permitted use, you will need to obtain permission directly from the copyright holder. To view a copy of this licence, visit <http://creativecommons.org/licenses/by/4.0/>.

© The Author(s) 2023